

## Investigation of Platinum-Doped TiO<sub>2</sub> Film $\lambda$ -Sensor

Jianxin Sheng, Nobuyuki Yoshida, Junichi Karasawa and Tatsuo Fukami

Faculty of Engineering, Shinshu University,  
500 Wakasato, Nagano 380, Japan

(Received November 22, 1995; accepted August 2, 1996)

**Key words:** alternate sputtering, TiO<sub>2</sub>:Pt film,  $\lambda$ -sensor, XPS shift, oxygen vacancy, catalytic effect

An abnormal electric property of TiO<sub>2-x</sub> film was observed during post-deposition heat treatment in order to demonstrate the effect of anion vacancies on the electric properties. X-ray photoemission spectra (XPS) of O<sub>1s</sub> and Ti<sub>2p(3/2)</sub> indicate that the shift and/or split of the core emission is related to anion vacancy. A thin film is preferable for fast response in terms of the observed thickness-dependent catalytic effect of rutile films. Alternately sputtered TiO<sub>2</sub>:Pt films display an improved electric performance.

### 1. Introduction

It is necessary in a combustion system to automatically control the air/fuel ratio of the inlet gases so as to minimize the fuel consumption and emission of harmful gases such as CO and NO<sub>x</sub>. In order to achieve this, an oxygen sensor is required to distinguish between the fuel-rich and fuel-lean mixtures on either side of stoichiometry. Intrinsic defects can easily be created in TiO<sub>2</sub>, particularly at elevated temperatures in the presence of reducing gases. TiO<sub>2</sub> is also known to have high diffusion coefficients for point defects in the bulk.<sup>(1,2)</sup> These features make rutile ceramics suitable as a potential oxygen sensor for monitoring fuel combustion.<sup>(3)</sup> Using thin film rather than ceramic material not only yields fast response but also makes it possible to combine a temperature-compensating film thermistor on the same substrate. Logothetis and Kaiser<sup>(4,5)</sup> have described an oxygen sensor based on a thick TiO<sub>2</sub> film grown by chemical vapor deposition using organometallics and were successful in improving the response.

In this work, thin rutile film prepared by magnetron sputtering was investigated to examine its applicability as a  $\lambda$ -sensor based on the evaluation of electric performance. Various parameters affecting the electric properties (*e.g.*, film thickness, electrode spacing

and catalytic metal) were evaluated. The anion vacancy-related electric behavior as well as the chemical state of the rutile film after interaction with reactive gases, *e.g.*, O<sub>2</sub> and CO, were also investigated for an atomistic understanding of the reversible solid-gas interaction.

## 2. Experimental

Rutile film with a thickness of 0.1~1.0  $\mu\text{m}$  was deposited on a corundum substrate by DC reactive magnetron sputtering. The conditions in Table 1 give rise to a pure rutile phase which has already been characterized in detail.<sup>(6)</sup> A pair of interdigital platinum electrodes patterned using a positive photoresist was deposited on the TiO<sub>2</sub> film in order to reduce the resistance (see Fig. 1). For catalytic metal doping, the rutile film was coated with 10% H<sub>2</sub>PtCl<sub>6</sub> solution and subsequently annealed at 600°C in air for 2 h to form a TiO<sub>2</sub>:Pt film (TP-A). Another (TiO<sub>2</sub>)<sub>0.7</sub>Pt<sub>0.3</sub> film (TP-B) was prepared by sputtering a coaxial Ti/Pt

Table 1  
Sputtering conditions.

Substrate	Corundum
Substrate temp.	550°C
Gas	100% O <sub>2</sub>
Pressure	20 mTorr
Time	1~8 h
Discharge current	200 mA
Power	120 W

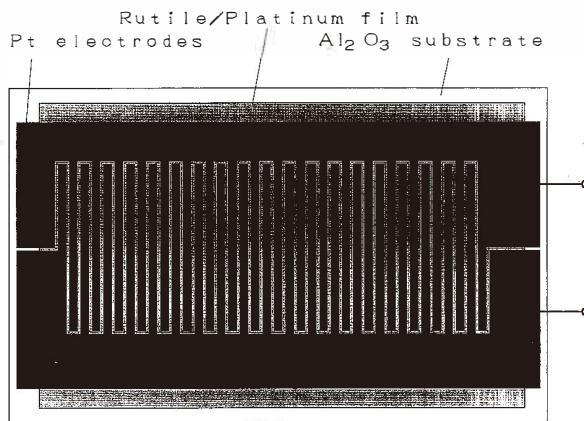


Fig. 1. Schematic diagram of TiO<sub>2</sub>:Pt film sensor on corundum (electrode spacing: 80  $\mu\text{m}$ ; substrate size: 16  $\times$  10 mm/mm).

target where the Ti and Pt plates were set for inner and outer sputtering, respectively.<sup>(6)</sup> The electric resistance was measured at different partial oxygen pressures adjusted using a CO/CO<sub>2</sub>-mixture for low P<sub>O<sub>2</sub></sub>, as well as an O<sub>2</sub>/Ar-mixture for high P<sub>O<sub>2</sub></sub>. The  $\lambda$ -characteristics were measured using a well-controlled laboratory apparatus, where the sensor element was exposed to a slowly flowing mixture of O<sub>2</sub> and CO with N<sub>2</sub> as the carrier gas at a total flow rate of ~500 ml/min and a flow velocity of ~3 cm/s. The O<sub>2</sub> flow alone was varied so as to create changeable air/fuel ratios (O<sub>2</sub>/CO in this case). As described previously,<sup>(7)</sup> in order to investigate the transient responses of the sensor, a 1 V supply voltage was applied across the series combination of the film sensor and a resistor R<sub>c</sub>. The sensor output V<sub>o</sub> measured across the resistor was recorded with the aid of a memory recorder (8820 MEMORY HI CORDER). The value of R<sub>c</sub> is approximately the geometrical mean of R<sub>ox</sub> and R<sub>re</sub>, which represent the resistances of the film sensor in oxidizing and reducing atmospheres, respectively. The temperature dependence of resistance for films 135, 270 and 810 nm thick was tested in 2% CO + N<sub>2</sub> gas to elucidate the thickness-related catalytic effect of rutile materials. In this experiment, electrodes with a spacing as wide as 1.2 mm were used to minimize the effect of the electrodes on the films. The chemical bonding state of rutile films under various conditions was ascertained by the XPS technique.

### 3. Results and Discussion

#### 3.1 Behaviors of oxygen vacancies in TiO<sub>2-x</sub> film

The variation in the resistance of an as-deposited rutile film while being heated is shown in Fig. 2. The result shows an abnormal change in resistance in the temperature range of 180~350°C. According to our previous AES investigations,<sup>(6)</sup> the as-deposited film is nonstoichiometric and has a considerable number of oxygen vacancies. This abnormal change in resistance is closely related to the nonstoichiometric composition of film. At low temperature (before point *a* in Fig. 2), the quasi free electrons required to preserve electric neutrality are bound to defect sites. With increasing the temperature, these trapped electrons are thermally agitated and become free, thus greatly modifying the electric conduction (point *a*→*b*). With further increase in temperature, the concentration of either V<sub>O</sub><sup>•</sup> or e' decreases rapidly because oxidation of the oxygen-deficient film gives rise to a stoichiometric composition. As a result, the resistance increases dramatically after point *b* until the film is fully oxidized at point *c*. The absence of such behavior in the annealed sample (see the cooling curve in Fig. 2) also suggests that this phenomenon can be attributed to oxygen vacancies. Point *b* does not definitely indicate either the point at which electron release finishes or the point at which TiO<sub>2-x</sub> oxidation starts. Two processes proceed simultaneously, of which electron release is dominant at an earlier stage, while the extinction of defects and quasi free electrons due to oxidation gradually dominates after point *b*, with the net effect of increasing the resistance.

If the fully oxidized sample in Fig. 2 is again treated in a reducing atmosphere at high temperature, the partially recovered V<sub>O</sub><sup>•</sup> number is not sufficiently large to show abnormal electric behavior, because TiO<sub>2-x</sub> heated in a reducing atmosphere, even up to 1000°C, only has an *x* value of 0.01<sup>(8)</sup> which is much smaller than the value of 0.4<sup>(6)</sup> in the as-deposited sample.

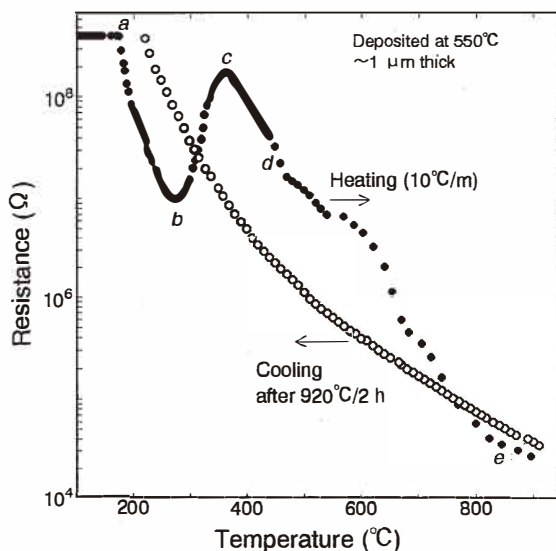


Fig. 2. Abnormal variation of resistance of freshly deposited  $\text{TiO}_{2-x}$  film during post deposition heating in air.

### 3.2 $P_{\text{O}_2}$ - and $l$ -sensing properties

Figure 3 shows the electric resistance of Pt-doped rutile film as a function of  $P_{\text{O}_2}$ .  $\text{TiO}_2$  exhibits  $n$ -type conduction in a wide range of  $P_{\text{O}_2}$ . At high  $P_{\text{O}_2}$ , the resistance varies as approximately the  $-1/6$  power of the  $P_{\text{O}_2}$  and shows  $p$ -type conduction. The  $n$ - $p$  transition point shifts toward the higher  $P_{\text{O}_2}$  area with increasing temperature. Similar phenomena have been observed in nondoped rutile film<sup>(6)</sup> and ceramics,<sup>(9)</sup> and have been attributed to the background acceptor impurities.

The excess air ratio  $\lambda$  (i.e., the normalized  $\text{O}_2/\text{CO}$  ratio) dependence of the resistance is shown in Fig. 4. In samples either with or without small intergranular catalytic Pt particles, a steplike change in the resistance occurs at precisely  $\lambda=1$ , indicating that  $\text{TiO}_2$  film, like  $\text{TiO}_2$ :Pt film, has catalytic properties sufficient to equilibrate the feed gas at the solid surface.  $\text{TiO}_2$ :Pt films show different electric characteristics depending on the preparation method. In addition to a higher sensitivity around  $\lambda=1$ , the TP-B film appears to be  $\lambda$ -sensitive even in the lean-burn area, unlike TP-A film or CVD-derived thick film<sup>(4)</sup> which have a constant resistance in this area and fail to show one-to-one correspondence between  $\lambda$  and resistance. Thus, the TP-B film may be of potential use in lean-burn detection, although the variation in resistance in this area is not as large as desired. Homogeneously dispersed platinum may be the reason for the improved electric characteristics of TP-B film.

Figure 5 shows the transient responses of rutile materials to lean-to-rich and rich-to-lean  $\lambda$ -switch pulses at around  $\lambda = 1$ . The following observation can be made.

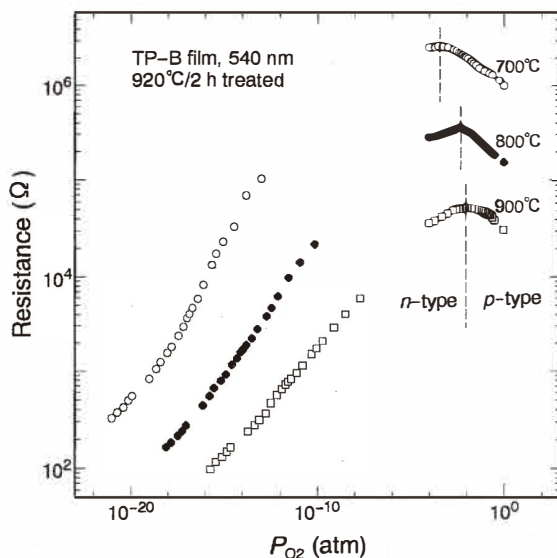


Fig. 3.  $P_{O_2}$  dependence of alternately deposited  $TiO_2$ : Pt film.

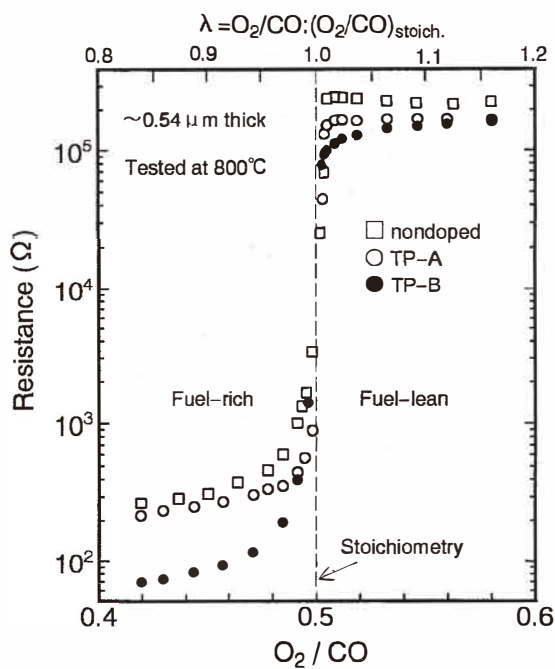


Fig. 4. Static  $\lambda$ -characteristics of □ pure  $TiO_2$ , ○  $H_2PtCl_6$ -impregnated  $TiO_2$  and ● sputtered  $TiO_2$ : Pt films.

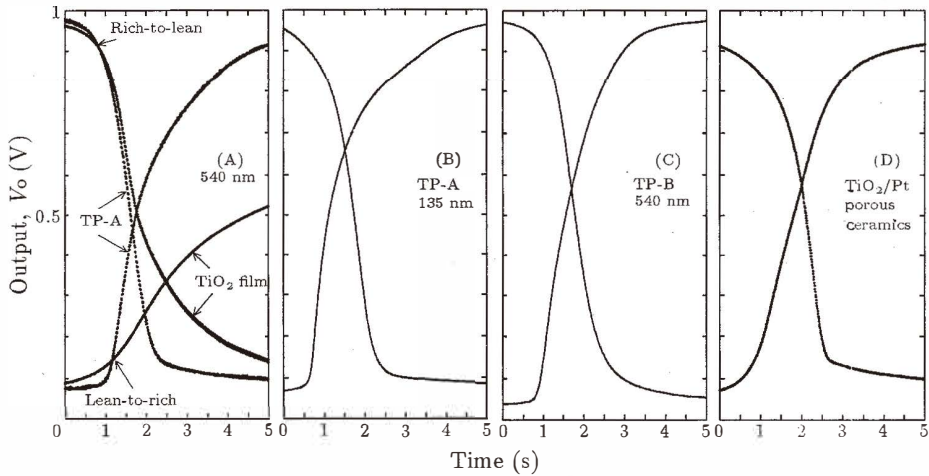


Fig. 5. Transient voltage responses of  $\text{TiO}_2$  film and ceramics to  $\lambda$ -switching pulses between 0.86 and 1.14. The experiments were performed at  $800^\circ\text{C}$ .

- (1) As seen in Fig. 5 (A), the response of nondoped film to lean-to-rich  $\lambda$ -switching is much slower than that of the reverse process. The addition of catalytic metal improves the response, particularly to the lean-to-rich pulse.
- (2) A decrease in the thickness of the TP-A films modifies the lean-to-rich response.
- (3) As expected from the difference in sensitivity shown in Fig. 4, the TP-B film shows a larger variation in output than that of TP-A film or  $\text{TiO}_2$  ceramics.
- (4) Both of the  $\text{TiO}_2$ : Pt films show a response superior to that of porous ceramics at the testing temperature, probably due to the short range of bulk diffusion.
- (5) The output of both TP-A and TP-B films is asymmetric. The response to a lean-to-rich pulse, for instance, shows an initial fast response followed by a slow approach to the steady state. This behavior may be related to the velocity boundary on the gas-solid interface. Since all gases are viscous, a boundary layer of thickness  $\delta$  of velocity gradient of gas flow will be formed on the solid surface. On the film surface, the gas velocity  $v_{\delta=0}$  is 0, and at a point far from the surface  $v_{\delta=\infty}$  equals  $v_0$ , i.e., the velocity of the ambient gas flow. If the ambient atmosphere is changed, the film sensor will respond to a continuous rather than a switchlike transient change in  $\lambda$  because of the relatively slow transport of gas through the boundary layer to the solid surface. As seen in Fig. 4, when  $\lambda$  passes through the 1.14~1.0 range, the film sensor gives no response at first, and then a drastic response as  $\lambda$  approaches 1.0; when  $\lambda$  passes 1.0 and moves towards 0.86, the sensor shows a continuous change in resistance and the voltage output slopes gently to reach a steady state, as indicated in Fig. 5.

The sensing mechanism of semiconducting oxide gas sensors, and  $\text{TiO}_2$  in particular, is usually understood atomistically in terms of the following steps:

- (a) Chemisorption and/or decomposition of gas molecules, *e.g.*, CO and  $\text{O}_2$ , on the surface

of the sensor.

- (b) Gas reaction with the aid of a catalyst to produce a localized equilibrium  $P_{O_2}$  around the sensor surface.  
 (c) The gas-solid binary phase defect reaction



changes the concentration of defects and electrons on the surface and, hence, changes the conduction of the material.

However, the above gas-solid defect reaction only takes place on the surface and at grain interfaces of the material and does not occur for bulk defects. Anion removal processes on the surface are considered to be sufficiently energetic to induce diffusion of  $V_O$  and  $e'$  into/out of the bulk oxide under the potential due to the concentration difference of the  $V_O$  and  $e'$  between the surface and bulk. This diffusion is important, because the self-arrangement of vacancies into/out of ordered and planar arrays is the dominant mechanism for the defect reaction going on throughout the bulk oxide.

### 3.3 Thickness dependence of catalytic activity

In nonequilibrium gas mixtures such as the products of combustion, the oxygen sensor is often required to sense the equilibrium oxygen pressure instead of the partial pressure of free oxygen, because in incomplete combustion, the former is always in one-to-one correspondence with the air/fuel ratio, whereas the latter fluctuates. In addition to the catalytic metal,  $TiO_2$  also contributes to the catalyzed oxidation of gas in the vicinity of the surface. The catalytic effect of pure  $TiO_2$  film has already been shown in Fig. 4. Additional information can be obtained by considering the thickness dependence of the resistance. In general, for samples with a fixed electrode pattern, the resistance of the film at a certain temperature and  $P_{O_2}$  should be inversely proportional to the film thickness  $d$  based on

$$R \propto d^{-1} \sigma^{-1} \propto d^{-1} P_{O_2}^{\frac{1}{n}} \exp\left(\frac{E}{kT}\right) \quad (2)$$

where  $n$  varies from 4 to 6 depending on the conduction mechanism, and  $\sigma$  is the conductivity of the film. This rule holds without exception for the thickness dependence of resistance in air. However, as seen in Fig. 6, the thickness dependence of resistance in 2.0% CO+N<sub>2</sub> gas shows a complicated pattern due to the catalytic oxidation on the solid surface between CO and the trace O<sub>2</sub> content in N<sub>2</sub>. At temperatures higher than 720°C, the catalytic ability of  $TiO_2$  is sufficiently high to generate a surrounding gas of equilibrium composition and hence the  $P_{O_2}$  for all samples is the same. Accordingly, the resistance is inversely proportional to the film thickness. However, the catalytic activity of  $TiO_2$  usually decreases with decreasing temperature and the gas around the sensor element tends to be nonequilibrium. At ~720°C, a step change in resistance occurs to produce an opposite thickness dependence of resistance, i.e., resistance increases with increasing thickness. According to eq. (2), it is clear that the nonequilibrium state is different for different samples, and that thinner films respond to a lower  $P_{O_2}$  than thicker ones, although all films were exposed to the same atmosphere. The difference in  $P_{O_2}$  is probably due to the different amount of catalytic oxidation of gases on the film surface. In other words, the

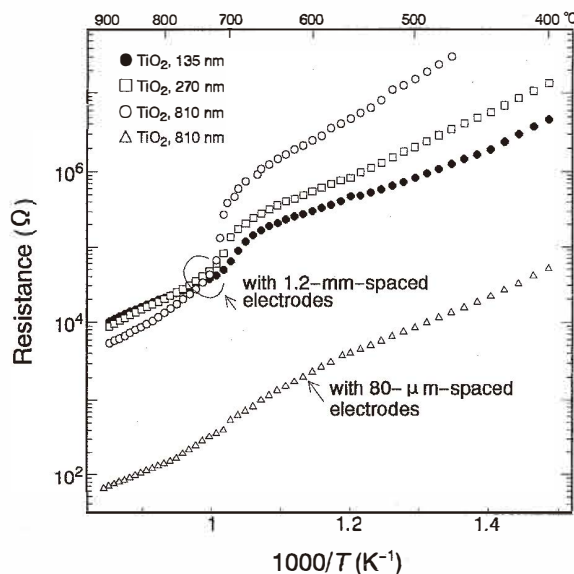


Fig. 6. Thickness and temperature dependence of resistance of rutile film in reducing atmosphere (2% CO+N<sub>2</sub>).

thinner film has a stronger catalytic effect and so it reacts with a lower  $P_{O_2}$  near the solid surface. Consequently the film has a lower resistance.

For interaction with reactive gases, intrinsic surface defects usually act as active sites for chemisorption and/or decomposition of the molecules.<sup>(10)</sup> Thus surface defects were considered to be the essential factor for the catalytic effect of TiO<sub>2</sub>. The observed difference in catalytic effect may be due to the fact that the thinner film has a unique defect structure which provides a favorable reaction path with a lower activation energy. However, relevant theories which support this hypothesis are not yet available. This issue must be clarified further.

As seen in Fig. 6, for samples mounted with electrodes 80  $\mu\text{m}$  apart, the drastic variation in resistance at around 720°C is not observed, because the equilibrium gas around the electrodes has a strong influence in the immediate vicinity and so the gas around the TiO<sub>2</sub> film is easily equilibrated.

### 3.4 Defect-related chemical bonding state

Figure 7(a) shows O<sub>1s</sub> core level emission from a freshly Ar<sup>+</sup>-etched surface. The arrows indicate the order of exposure. Spectra for as-deposited and reduced samples show a main peak at around 531 eV and a secondary peak on the high-energy side at around 534 eV, while the spectrum for the oxidized sample shows only a single peak. As a rule, the existence of a secondary peak around the main emission suggests a variety in the chemical environments, such as the coordination state of atoms. In the as-deposited sample, the

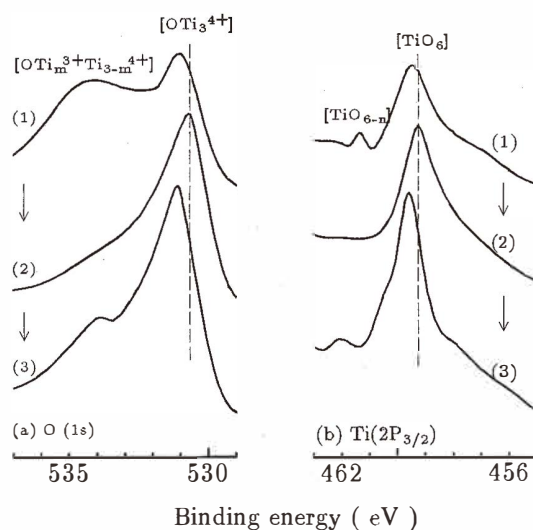


Fig. 7. Photoemission spectra of (a)  $O_{1s}$  and (b)  $Ti_{2p(3/2)}$  from  $TiO_{2-x}$  films (1) as-deposited, (2) oxidized at  $700^\circ\text{C}$  and (3) deoxidized in 10%  $\text{CO}+\text{N}_2$  at  $700^\circ\text{C}$ . The expression in square brackets indicates the coordination state.

suboxide, the structure of which was confirmed by AES, may be regarded as a solid solution of  $TiO_2$  and low-valence oxides, *e.g.*,  $Ti_3O_5$  and  $Ti_2O_3$ . The main peak is ascribed to  $O^{2-}$  ions of the normal oxide lattice, while the secondary peak is evidently associated with the  $O^{2-}$  ions partially coordinated by  $Ti^{3+}$  ions, rather than chemisorption products such as hydroxide and carbonate. In the fully oxidized sample, all of the  $O^{2-}$  ions are in the same chemical environment, hence the absence of the secondary peak. If the oxidized film is retreated in a reducing atmosphere, as shown in Fig. 7(a)(3), the secondary peak appears again, although its intensity is much lower than that for the as-deposited sample. The difference in intensity may be attributed to the difference in the extent of nonstoichiometry, as mentioned earlier.

As seen in Fig. 7(b), the spectra for  $Ti_{2p(3/2)}$  are quite similar to those for  $O_{1s}$ . The high concentration of oxygen vacancies in the as-deposited or reduced samples leads to a slight shift in the  $Ti_{2p(3/2)}$  core emission at around 460.5 eV to lower binding energies than those in the fully oxidized sample. This phenomenon agrees well with the results of earlier studies<sup>(10)</sup> in which defects on  $TiO_2$  (110) single crystal induced by  $\text{Ar}^+$ -ion bombardment caused a similar shift of the  $Ti_{2p(3/2)}$  peak. Furthermore, in the rutile structure,  $Ti^{4+}$  ions are octahedrally coordinated, and the structure can be regarded as consisting of  $[TiO_6]$  octahedra which share edges and corners in such a way that each oxygen ion belongs to 3 octahedra. When a bridging  $O^{2-}$  ion is removed to form an oxygen vacancy, three neighboring octahedra become fivefold coordinated. This defect complex is expressed as  $3Ti^{4+} \cdot V_O$ . If two electrons are trapped at the defect, two  $Ti^{4+}$  ions are reduced to  $Ti^{3+}$  and

the defect configuration may be denoted as  $\text{Ti}^{4+} \cdot 2\text{Ti}^{3+} \cdot V_{\text{O}}^{\bullet\bullet}$ . Titanium ions in the defect complex and in the normal sites have a distinct chemical environment and, consequently, different binding energies. The observed  $\text{Ti}_{2p(2/3)}$  emission, therefore, can be interpreted as consisting of two components, one due to normal  $\text{Ti}^{4+}$  ions coordinated to  $\text{O}^{2-}$  ions (the lower-binding-energy feature), and another due to titanium ions partially associated with oxygen vacancies (the secondary feature at around 461.5 eV). A similar phenomenon has been observed for  $\text{Ba}^{2+}$  ions in  $\text{YBa}_2\text{Cu}_3\text{O}_{6,9}$  superconductor.<sup>(11)</sup> The difference in the binding energy of the two components is related to the polarization of the oxygen vacancy. For the same reason as that given for  $\text{O}_{1s}$  emission, the secondary feature of  $\text{Ti}_{2p(3/2)}$  disappears after oxidation, as seen in Fig. 7(b)(2).

#### 4. Conclusions

The variation in conduction during post-deposition heat treatment of freshly deposited films confirms that the conduction of  $\text{TiO}_2$  is closely associated with nonstoichiometric defects. This phenomenon, combined with the observed chemical bonding state, helps us understand the behavior of  $V_{\text{O}}$  in  $\text{TiO}_2$  films in oxidizing or reducing atmospheres. Thin films are favorable for the improvement of electrical response from the viewpoint of thickness dependence of the catalytic activity and the bulk diffusion process. Platinum electrodes with small spacing also contribute to the gas equilibrium on the surface of  $\text{TiO}_2$  film. A dramatic change in resistance occurring at exactly  $\lambda=1$  with a fast response proves rutile film to be a promising oxygen-sensing material. Alternately sputtered  $\text{TiO}_2$ :Pt film can modify the electric performance at around  $\lambda=1$ . Since the electric output of a  $\text{TiO}_2$  film sensor depends on the temperature, as well as on the partial oxygen pressure of the surroundings, the effect of temperature on the sensor should be minimized by means of a compensation system. We are now in the process of examining *p*-type spinel  $\text{ZnCr}_2\text{O}_4$  film as a compensating thermistor which will be reported elsewhere.

#### References

- 1 R. Haul and G. Dumbgen: *J. Phys. Chem. Solids* **26** (1965) 1.
- 2 A. Hippel, J. Kalnajs and W. Westphal: *J. Phys. Chem. Solids* **23** (1962) 779.
- 3 A. L. Micheli: *Amer. Ceram. Bull.* **63** (1984) 694.
- 4 E. M. Logothetis and W. J. Kaiser: *Sensors and Actuators* **4** (1983) 333.
- 5 W. J. Kaiser and E. M. Logothetis: U.S. Patent, 4,504,522.
- 6 J. Sheng, N. Yoshida, J. Karasawa and T. Fukami: *Proc. 3rd International Symposium on Sputtering & Plasma Processes* (Tokyo, Japan, 1995) p. 367.
- 7 J. Sheng and T. Fukami: *Sensors and Materials* **7** (1995) 361.
- 8 P. Kofstad: *Nonstoichiometry, Diffusion, and Electric Conductivity in Binary Metal Oxides* (Krieger Publishing, USA, 1983) p. 141.
- 9 U. Balachandran, N. Eror: *J. Material Science* **23** (1988) 2676.
- 10 W. Gopel and G. Rucker: *Phys. Rev.* **28** (1983) 3427.
- 11 H. M. Meyer, Y. Gao, T. J. Wagener and J. H. Weaver: *American Institute of Physics Conference Proceedings No.165*, eds., J. Harper, R. Colton and L. Feldman (New York, 1987) p. 259.